Metal-Free Deoxygenation of Amine N -Oxides: Synthetic and Mechanistic Studies

William Lecroq, Jules Schleinitz, Mallaury Billoue, Anna Perfetto, Annie-Claude Gaumont, Jacques Lalevée, Ilaria Ciofini, Laurence Grimaud, Sami Lakhdar

Metal-Free Deoxygenation of Amine *N*–Oxides: Synthetic and Mechanistic Studies

William Lecroq,[a, ‡] Jules Schleinitz,[b, ‡] Mallaury Billoue,[a] Anna Perfetto,[c] Annie–Claude Gaumont,[a] Jacques Lalevée,[d] Ilaria Ciofini,[c] Laurence Grimaud,*[b] and Sami Lakhdar*[e]

Dedicated to memory of Prof. Jean-Michel Savéant

[a] Dr. W. Lecroq, M. Billoue, Prof. Dr. A.–C. Gaumont and Dr. S. Lakhdar
Normandie Univ., LCMT, ENSICAEN, UNICAEN, CNRS,
6, Boulevard Maréchal Juin, Caen 14000 France
E-mail: lakhdar@chimie.ups-tlse.fr
[b] J. Schleinitz and Dr. L. Grimaud
Laboratoire des biomolécules, LBM, Département de chimie, École normale supérieure, PSL University, Sorbonne Université, CNRS, 75005 Paris, France.
E-mail : laurence.grimaud@ens.psl.eu
[c] Ms. A. Perfetto and Dr. I. Ciofini
Institute of Chemistry for Life and Health Sciences (i-CLeHS), Chimie ParisTech, PSL University, CNRS,
11 rue P. et M. Curie, F-75005 Paris, France
[d] Prof. Dr. J. Lalevée
Université de Haute-Alsace, CNRS, IS2M UMR 7361, F-68100 Mulhouse, France
[e] Dr. S. Lakhdar
Université Paul Sabatier, Laboratoire Hétérochimie Fondamentale et Appliquée (LHFA, UMR 5069),
118 Route de Narbonne, 31062, Toulouse Cedex 09, France
E-mail : lakhdar@chimie.ups-tlse.fr
[‡] These authors contributed equally to this work.

Supporting information for this article is given via a link at the end of the document.

Abstract: We report herein an unprecedented combination of light and P(III)/P(V) redox cycling for the efficient deoxygenation of aromatic amine N-oxides. Moreover, we discovered that a large variety of aliphatic amine N-oxides can easily be deoxygenated by using only phenylsilane. These practically simple approaches proceed well under metal–free conditions, tolerate many functionalities and are highly chemoselective. Combined experimental and computational studies enabled a deep understanding of factors controlling the reactivity of both aromatic and aliphatic amine N-oxides.

Introduction

Trivalent organophosphorus compounds such as phosphines find widespread use throughout numerous fields of synthetic chemistry. Indeed, apart from their use as ligands in transition metal catalysis or as organocatalysts, phosphanes have been widely employed as stoichiometric reagents in various synthetic transformations such as Wittig, Appel, Staudinger or Mitsunobu reactions, to name a few.[1] The driving force for all these transformations is the formation of high molecular weight phosphine oxide as a byproduct, which poses separation and waste disposal problems. Thus, the development of catalytic variants of these reactions in organophosphorus reagent and utilizing alternative feedstocks is highly important.[2] In this context, the use of silanes as reducing agents of phosphine oxides has appeared as an efficient solution enabling the development of numerous interesting phosphane–catalyzed processes.[3] Remarkably, in these polar reactions, the silane reacts selectively with phosphine oxide and not with other reagents present in the media.[4] While the P(III)↔P(V) redox cycling approach has been frequently used in polar organic reactions, it has, to the best of our knowledge, never been applied to photoinduced processes, where phosphanes are used in stoichiometric amounts.[5] This could be explained by the ability of radicals, generated under photoinduced conditions, to react with silanes through hydrogen atom transfer of Si–H bonds, thus preventing the reduction of phosphine oxide to recover the phosphine.

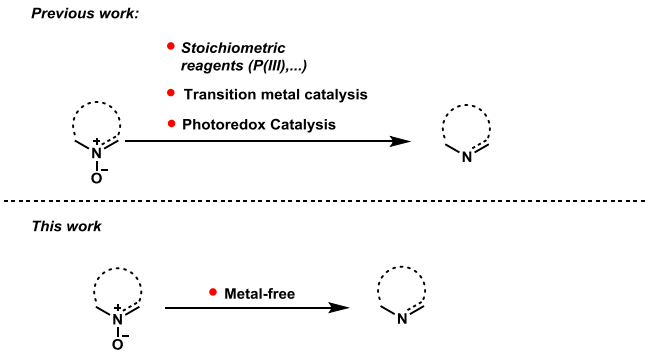

Scheme 1. Deoxygenation of Amine *N*–oxides.

However, as many photochemical processes are known to involve electronically neutral transient intermediates, we reasoned that P(III)↔P(V) redox cycling might be applicable for those reactions. In this context, the deoxygenation of heteroaromatic N–oxides has captured our attention because of: *i*) its great importance in various areas[6]ranging from synthesis to catalysis[7]and biology[8], ii) the non–catalyzed version requires a large amount of phosphane and proceeds at high temperature;[9] iii) previous physical

organic studies postulated the formation of oxaziridine intermediate upon excitation of heteroaromatic N–oxides with light.[10] This highly reactive intermediate should react fast with phosphane to give the heteroaromatic compound along with phosphine oxide. Based on this and on the fact that phosphanes are more nucleophilic than silanes,[11]we assumed silane would reduce the in situgenerated phosphine oxide rather than reacting with the oxaziridine. Extension of this approach to aliphatic amine N-oxide will also be investigated (Scheme 1).

Results and Discussion

To test this hypothesis, we investigated the deoxygenation of 4–cyanopyridine N–oxide **1a** in the presence of a catalytic amount of phosphine oxide **2**, phenylsilane as a reducing agent, in different solvents and under blue light irradiation.

Table 1. Optimization of the reaction conditions.[a]

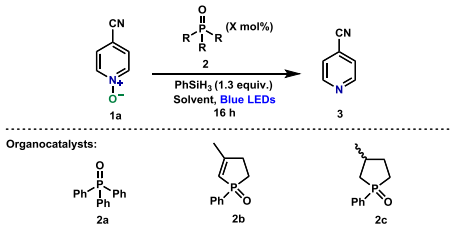

Entry	Organocatalyst (X mol %)	Solvent	Yield [%][b]
1	**2a** (20)	CH_3CN	0
2	**2b** (20)	CH_3CN	99
3	**2c** (20)	CH_3CN	99
4	**2b** (20)	CH_2Cl_2	8
5	**2b** (20)	Toluene	traces
6	**2b** (20)	DMF	2
7	**2b** (10)	CH_3CN	99
8	**2b** (5)	CH_3CN	93
9	**2b** (2.5)	CH_3CN	83
10	**–**	CH_3CN	0
11	**2b** (10)	CH_3CN	0[c]
12	**2b** (10)	CH_3CN	traces[d]
13	**2b** (10)	CH_3CN	99[e]

[a] Reaction conditions: 1a (0.5 mmol, 1 equiv.), phenylsilane (0.65 mmol, 1.3 equiv.), organocatalyst (X mol %), solvent (5 mL), 16h. [b] NMR yields are determined via 1H NMR spectroscopy vs internal standard. [c] In the absence of phenylsilane. [d] In the absence of light. [e] The Schlenk-flask was irradiated through a cut off filter ([$NaNO_2$] = 0.72 M in aqueous solution, transparent for light > 385 nm).

As depicted in Table 1, while triphenylphosphine oxide (**2a**, 20 mol%) failed to catalyze the reaction (entry 1) in acetonitrile, phosphine oxides **2b** and **2c** gave the desired product in excellent yields (entries 2-3, 99%). This might be attributed to the ability of cyclic phosphine oxides to be easily reduced by silanes compared to the acyclic ones.

It should be mentioned that a seminal study by Scaiano *et al*. showed the efficiency of triethylphosphite to deoxygenate pyridine N-oxide in acetonitrile under UV irradiation (λ_{max} = 325 nm).[6a]

When the same phosphite was used under our conditions (λ_{max} = 420 nm), no reaction was observed (see supporting information).

Based on these first results, the commercially available 3-methyl-1-phenyl-phospholane oxide **2b** was used for optimization. In this context, a solvent screening including dichloromethane, toluene and DMF (entries 4–6) showed a very low conversion compared to acetonitrile (entry 2). While lowering the catalyst loading to 10 mol % (entry 7, 99%) did not affect the performance of the reaction, reducing it to 5 and 2.5 mol% diminished the yield of the reaction (93% and 83%, respectively, entries 8-9). Interestingly, the organocatalyst (**2b**, entry 10), phenylsilane (entry 11) and light (entry 12) were found to be essential for the deoxygenation reaction as no conversion was observed in their absence. Finally, to exclude the involvement of UV light, we irradiated the sample through a UV filter (75% w/v $NaNO_2$ solution, cut-off: λ =385 nm) and a nearly full conversion has been attained (entry 13, 99%). With the optimized conditions in hand, we next investigated the scope of the photoreaction.

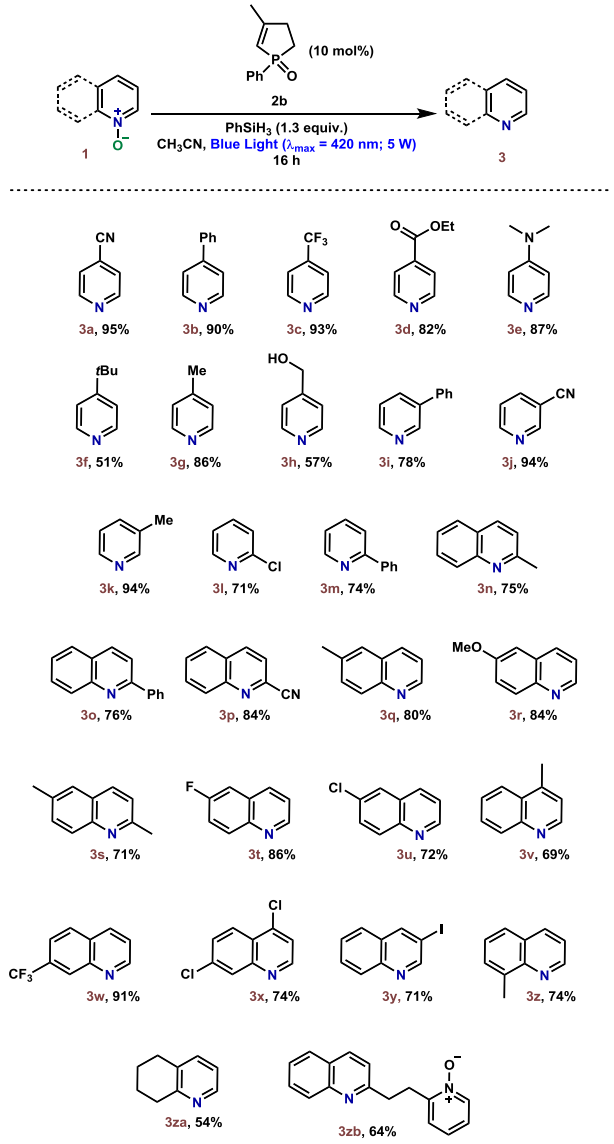

Figure 1. Scope of the photochemical deoxygenation of heteroaromatic *N*–oxides. Reaction conditions: **1** (0.5 mmol, 1 equiv.), phenylsilane (0.65 mmol, 1.3 equiv.), **2b** (10 mol %), acetonitrile (5 mL), Blue LEDs (5 W), 16h.

As shown in Figure 1, the reaction proceeds well with pyridine *N*–oxides *para*-substituted with either electron–withdrawing (**3a–d**) or electron–rich (**3e–h**) groups in good to excellent yields. Pyridine *N*–oxides bearing substituents at the *meta* (**3i–k**) or *ortho* (**3l,m**) positions can be smoothly deoxygenated under the optimized conditions. Notably, different functional groups (CF_3 (**3c**, 93%), CO_2Et (**3d**; 82%), CH_2OH (**3h**; 57%), CN (**3j**; 94%) and chloride (**3l**; 71%)) on the aromatic rings were well-tolerated. Similarly, a large variety of quinoline oxides, bearing different electronic substituents on the aromatic and/or heteroaromatic rings (**3m–3v**), performed well under the optimized reaction conditions, affording the corresponding reduced heterocycles in good to excellent yields (69–94%). 5,6,7,8-tetrahydroquinoline–*N*–oxide can also be deoxygenated to the corresponding quinoline **3za** in fair 54% yield.

More importantly, when starting with a bis–*N*–oxide, bearing both a quinoline and a pyridine *N*-oxides, only the former is deoxygenated under our photochemical conditions and the pyridine *N*–oxide (**3zb**) was deoxygenated using 1.3 equiv of silane affording 3zb in 64% yield. It should be noted that a similar chemoselective approach has recently been reported by Kim and Lee, where $[Ru(bpy)_3]$-$Cl_2{}^{\bullet}6H_2O$ was used as a photocatalyst in the presence of excess of hydrazine hydrate, which serves as reductive quencher and hydrogen source.[6g]

To evaluate the general applicability of this photoorganocatalytic approach, we investigated the deoxygenation of dialkylarylamine *N*-oxide (Figure 2).

When optimizing the deoxygenation of *N*,*N*-dimethyl aniline *N*–oxide, we were surprised to find that the reaction takes place smoothly in the absence of both light and organocatalyst (**2b**). By combining various aniline *N*–oxides and phenylsilane (1.3 equiv.) in acetonitrile the corresponding anilines (**5a–5g**) can be obtained within 10 min in very good yields (82–92%). Similarly, the deoxygenation of a series of *N*-benzylpyrrolidine *N*-oxides, bearing electron -donating and -withdrawing substituents on the aromatic rings, works smoothly, delivering the amines (**5h–5l**) in yields ranging from 59 to 87%. The deoxygenation of Rhodamine B *N*–oxide can easily be performed under the optimized conditions to yield the fluorescent dye **5m** in good yield (83%).

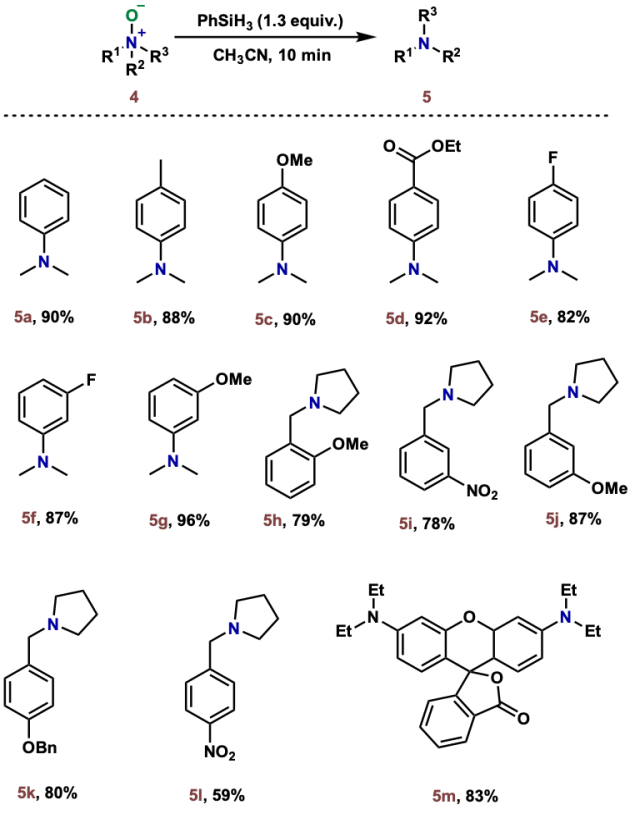

Figure 2. Scope of the photochemical deoxygenation of aliphatic amine *N*–oxides. Reaction conditions: **4** (0.5 mmol, 1 equiv.), phenylsilane (0.65 mmol, 1.3 equiv.), acetonitrile (5 mL).

Mechanistic Investigations

In order to gain insights into the reaction mechanism of the photo-deoxygenation of amine *N*–oxides (Figure 1), complementary experimental and computational studies were performed.

We first focused our attention on the reaction mechanism of deoxygenation of *N*-heterocyclic *N*-oxides.

In order to confirm the generation of 3-methyl-1-phenyl-phospholane (**7**) during the reaction, we reacted 3-methyl-1-phenyl-phospholane oxide (**2b**) with phenylsilane under blue light irradiation. As shown in Figure S1, almost 50% of the phosphane was detected by ^{31}P NMR spectroscopy after 16 h of irradiation. Importantly, 30% and 70% of **7** were obtained when the same reaction was carried out in the dark at room temperature and at 70 °C, respectively. These results indicate that the reduction of **2b** by phenylsilane is presumably a thermally driven process. Noteworthy mentioning, the reaction of 3-methyl-1-phenyl-phospholane (**7**, 1 equiv.) with 4–cyanopyridine *N*–oxide (**1a**, 1.2 equiv.) under blue irradiation gives rise to 4-cyanopyridine (**3a**) in 92% yield, which revealed the intermediacy of phospholane (**6**) in the catalytic reaction.

We next turned our attention to ascertain the nature of the photoactive species involved in photodeoxygenation of 4–cyanopyridine *N*–oxide (**1a**). To this end, we performed UV−vis spectroscopic measurements on various combinations of **1a**, **7** and phenylsilane in dichloromethane for each species (Figures S2–S4, supporting information). Besides the pyridine *N*-oxide **1a** that absorbs slightly in the visible region, all of the other components are silent in this region (> 390 nm). Furthermore, addition of **7** did not induce any bathochromic shift to the spectrum of **1a**, ruling out the formation of an electron donor-acceptor complex (EDA).[14]

These findings are consistent with simulated UV–visible spectra reported in the supporting information (Figure S5). On this basis, we assume a photo-activation of the pyridine *N*-oxide (**1a**) leading to the formation of the (**1a**)* species. In aprotic solvents, two scenarios can next be envisaged (Scheme 2): *i*) a photoisomerization leading to the formation of an unstable fused oxaziridine **6a**, which can further react with **7** to yield the pyridine **3a**, or *ii*) a single electron transfer from the phosphane (**7**) to (**1a**)* to generate the phosphoniumyl radical (**7**)$^{\bullet+}$ along with the reduced pyridine *N*–oxide species (**1a**)$^{\bullet-}$ (Scheme 2, grey arrows).

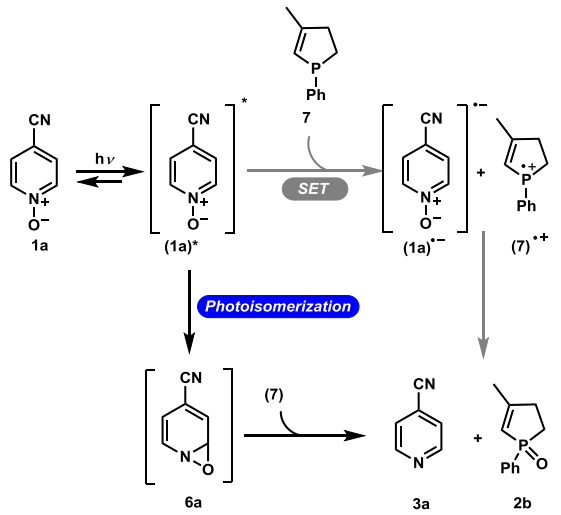

Scheme 2. Working mechanistic hypotheses for the deoxygenation of 4–cyanopyridine *N*–oxide (**1a**).

Even if both reaction mechanisms have been previously postulated in literature,[15] experimental evidence of the formation of oxaziridine intermediates could be observed only in a few cases since many heteroaromatic *N*-oxides do not show transient absorption by laser flash photolysis.[10] We then turned our attention to theoretical approaches to provide valuable insights.

To investigate the two possible reaction mechanisms, we resorted on Density Functional Theory (DFT)[16] and Time Dependent DFT[17] (as detailed in SI) to model ground and excited state reactivity. First, to assess the photoisomerization hypothesis, we computed the ground and excited state potential energy surfaces (PES) describing the formation of the oxaziridine intermediate (**6a**) from **1a**, as this is supposed to be the key step of the process.

As relevant structural parameters, two angles (α and β in Figure 3) were considered. These two angles describe respectively, the closure of the CNO ring and the out of plane position of the O atom with respect to the heteroaromatic ring.

As shown in Figure 3, the minima corresponding to **1a** and **6a** can be located on the ground state (S_0), the latter corresponding to an α=56.8° and β=-107.7°, characteristic of the oxaziridine geometry. Analysis of the ground and excited state PES reveals the presence of a region, close to the transition state of the ground state, with a small difference in energy (~5 kcal/mol) between S_1 and S_0. In this region, relaxation from the excited to the ground state is likely to occur. On this basis, we can reasonably assume the photoisomerization reaction occurs following a four-step isomerization mechanism: after vertical absorption leading to the population of the S_1 excited state (step 1, dashed blue arrow), vibrational relaxation leads to the S_1 energy minimum (step 2, red arrow) and if sufficient energy is provided, the region of $S_1 \rightarrow S_0$ vertical decay can be reached (step 3, dashed black arrow) yielding the oxaziridine which can finally vibrationally relax toward its corresponding minimum at the ground state (step 4, blue arrow).

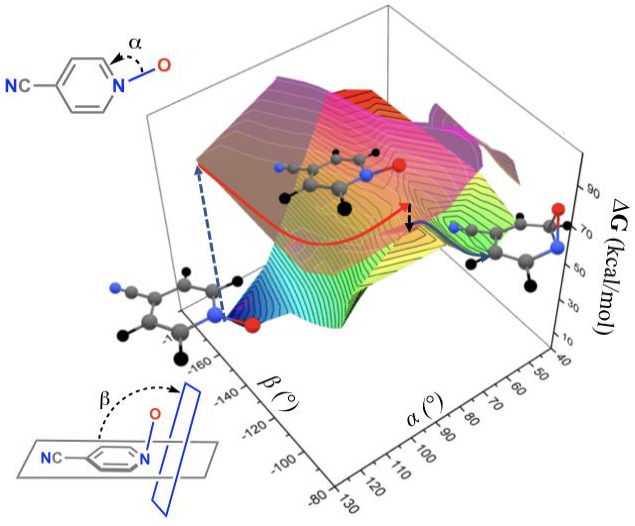

Figure 3. S_0 and S_1 free energy surfaces for the 4-cyano pyridine *N*-oxide (**1a**).

Using this mechanistic modeling (full details in the supporting information), we were able to quantify free energy difference ($\Delta G_{S1\text{-}oxa}$) between the *N*-oxide first excited state minimum and the oxaziridine intermediate on the ground state PES, and activation energy ($\Delta G^{\neq}_{oxa}$) for the rate determining step of the photocyclization *i.e.* the isomerization process from the first excited state minimum of the *N*-oxide to the oxaziridine (step 2 to step 3). From these data, the reaction of **1a** is thermodynamically favoured ($\Delta G_{S1\text{-}oxa}$ = -43.6 kcal/mol) and kinetically feasible at room temperature ($\Delta G^{\neq}_{oxa}$ = 5 to 8 kcal/mol).

In order to test the single electron transfer mechanism displayed in Scheme 2 we applied Marcus theory[18] (details in the supporting information) to compute both activation and reaction energies (reported in Table 2). This pathway was found to be kinetically ($\Delta E^{\neq}_{SET}$ = 2.24 kcal/mol) and thermodynamically feasible (ΔE_{SET} = -29.2 kcal/mol). However, a direct comparison between both mechanisms was not possible because of the difficult evaluation of the entropic contribution.[19]

To overcome this issue we applied the same methodology to three additional substrates, the electron–rich *N',N'*–dimethylaminopyridine *N*–oxide (**1e**) giving **3e** in high yield and two acridine *N*–oxides **1zc** and **1zd**, which failed to react under the optimized experimental conditions (Figure 1). The results presented in Table 2 show that, if SET is computed to be feasible in all cases, it is found to be more favorable with acridine *N*–oxide **1zd** than with the pyridine *N*–oxide **1e**, which disagrees with experimental results. The formation of the oxaziridine intermediate is favored in the case of **1a,e** showing the smallest activation energies, while deoxygenation of **1zc,d** is expected to be unlikely to occur and indeed did not proceed under our optimized conditions. On this basis, the computed photoisomerization mechanism is consistent with the observed yields.

Table 2. Computed Free energies ($\Delta G_{S1\text{-}oxa}$ and ΔE_{SET}) activation energies ($\Delta G^{\neq}_{oxa}$ and $\Delta E^{\neq}_{SET}$) associated to the photoisomerization yielding to the oxaziridine formation (oxa) and the single electron transfer mechanism (SET). Refer to Scheme 2 for detail.

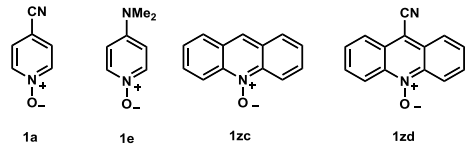

1a 1e 1zc 1zd

Substrate	$\Delta G_{S1\text{-}oxa}$ (kcal/mol)	$\Delta G^{\neq}_{oxa}$ (kcal/mol)	ΔE_{SET} (kcal/mol)	$\Delta E^{\neq}_{SET}$ (kcal/mol)
1a	–43.61	5 to 8	–29.20	2.24
1e	–39.94	2 to 6	5.95	10.54
1zc	–15.26	18 to 22	–4.69	9.97
1zd	–11.29	20 to 24	–15.67	2.58

Finally, the mechanism of deoxygenation of dialkylarylamine *N*-oxide remains to be elucidated. To this end, we considered the reaction of phenylsilane with the parent pyridine *N*–oxide and with *N*,*N*-dimethyl aniline *N*–oxide **4a**.

In both cases, a pre-complex between phenylsilane and amine *N*–oxide (**1**, **4a**) is formed, the oxygen coordinated to the silicon atom of the phenylsilane (detailed pathway is reported in the supporting information).

In the case of **4a** the energetic barrier to overcome for the formation of the final product is found to be 18.6 kcal/mol. The optimized transition state structure (TS_a) shows that the oxygen atom is bridging the nitrogen, the silicon and the hydrogen atoms (O–N = 1.73 Å, O–Si = 1.76 Å, O–H = 1.66 Å) with a N-O-H quasi linear arrangement. Though the reaction in the case of the pyridine *N*-oxide **1** proceeds *via* a similar transition state (TS_b), the energy required for this reaction is around 20 kcal/mol higher than that for the reaction of **4a** with phenyl silane in agreement with the experimental observation of the failure of pyridine *N*-oxides to react with phenylsilane at room temperature. The difference of reactivity between **1** and **4a** stems to higher energy NO bond in the latter compared to the former, due to conjugation with the heterocycle.

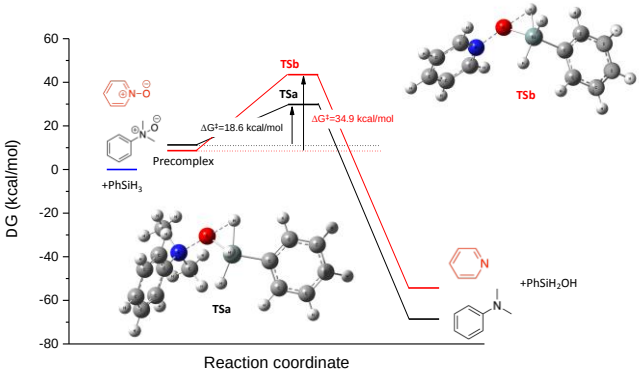

Figure 4. DFT–calculated Gibbs energy profiles for the reactions of phenylsilane with **1** and **4a**, respectively.

Conclusion

In summary, this work demonstrates the efficiency of P(III)↔P(V) redox cycling with light to drive practically simple deoxygenation of a large variety of heteroaromatic *N*–oxides. Expensive and highly sensitive catalysts, which are typically combined with phenylsilane to reduce dialkylarylamine *N*-oxides, turned out to be not required as such a deoxygenation proceeded within 10 minutes at room temperature. In order to understand factors controlling both reactions, DFT calculations have been performed. It was shown that the photochemical deoxygenation proceeds most likely through the formation of a transient fused oxaziridine as a key intermediate that reacts with phosphane to yield the heteroarene. The reaction of dialkylarylamine *N*-oxides with phenylsilane occurs according to a concerted pathway, with an activation energy lower than that calculated for the deoxygenation of pyridine *N*–oxide with

phenylsilane. Given the importance of deoxygenation of amine *N*–oxides in different domains going from catalysis to biology, these simple approaches should find wide applications.

Experimental Section

Experimental Details (see supporting information).

Acknowledgements

The authors thank the CNRS, Normandie Université, Région de Normandie, Labex Synorg (ANR-11-LABX-0029), ENSCP Chimie ParisTech, ENS, PSL for financial support. IC and AP acknowledge support from the European Research Council (ERC) for funding under the European Union's Horizon 2020 research and innovation program (grant agreement No 648558, STRIGES CoG grant).

Keywords: deoxygenation • mechanisms • photochemistry • organocatalysis • selectivity

[1] H. Guo, Y. C. Fan, Z. Sun, Y. Wu, O. Kwon, *Chem. Rev.* **2018**, *118*, 10049–10293.

[2] S. Xu, Z. He, *RSC Adv.* **2013**, *3*, 16885–16904.

[3] For selected contributions, see: a) C. J. O'Brien, J. L. Tellez, Z. S. Nixon, L. J. Kang, A. L. Carter, S. R. Kunkel, K. C. Przeworski, G. A. Chass, *Angew. Chemie - Int. Ed.* **2009**, *48*, 6836–6839. b) K. Fourmy, A. Voituriez, *Org. Lett.* **2015**, *17*, 1537–1540. c) W. Zhao, P. K. Yan, A. T. Radosevich, *J. Am. Chem. Soc.* **2015**, *137*, 616–619. d) M. L. Schirmer, S. Adomeit, T. Werner, *Org. Lett.* 2015, **17**, 3078–3081. e) X. Han, N. Saleh, P. Retailleau, A. Voituriez, *Org. Lett.* **2018**, *20*, 4584–4588. f) T. V. Nykaza, J. C. Cooper, G. Li, N. Mahieu, A. Ramirez, M. R. Luzung, A. T. Radosevich, *J. Am. Chem. Soc.* **2018**, *140*, 15200–15205. g) T. V. Nykaza, A. Ramirez, T. S. Harrison, M. R. Luzung, A. T. Radosevich, *J. Am. Chem. Soc.* **2018**, *140*, 3103–3113. h) L. Longwitz, A. Spannenberg, T. Werner, *ACS Catal.* **2019**, *9*, 9237–9244. i) C. Lorton, T. Castanheiro, A. Voituriez, *J. Am. Chem. Soc.* 2019, **141**, 10142–10147. j) L. Longwitz, T. Werner, *Pure Appl. Chem.* **2019**, *91*, 95–102. k) A. Ghosh, M. Lecomte, S. H. Kim-Lee, A. T. Radosevich, *Angew. Chemie - Int. Ed.* ***2019***, *58*, 2864–2869. l) L. Longwitz, T. Werner, *Angew. Chemie - Int. Ed.* **2020**, *59*, 2760–2763.

[4] For a recent review, see: A. Voituriez, N. Saleh, *Tetrahedron Lett*. **2016**, *57,* 4443–4451.

[5] For selected articles, see: a) E. E. Stache, A. B. Ertel, T. Rovis, A. G. Doyle, *ACS Catal.* **2018**, *8*, 11134–11139. b) M. Zhang, X. A. Yuan, C. Zhu, J. Xie, *Angew. Chemie - Int. Ed.* **2019**, *58*, 312–316. c) P. J. Xia, Z. P. Ye, Y. Z. Hu, D. Song, H. Y. Xiang, X. Q. Chen, H. Yang, *Org. Lett.* **2019**, *21*, 2658–2662. d) J. I. Martinez Alvarado, A. B. Ertel, A. Stegner, E. E. Stache, A. G. Doyle, *Org. Lett.* **2019**, *21*, 9940–9944. e) Y. Q. Guo, R. Wang, H. Song, Y. Liu, Q. Wang, *Org. Lett.* **2020**, *22*, 709–713.

[6] a) G. Bucher, J. C. Scaiano, *J. Phys. Chem*. **1994**, *98*, 12471–12473. b) J. Jeong, K. Suzuki, M. Hibino, K. Yamaguchi, N. Mizuno, *ChemistrySelect* **2016**, *1*, 5042–5048. c) F. Ding, Y. Jiang, S. Gan, R. L. Y. Bao, K. Lin, L. Shi, *European J. Org. Chem.* **2017**, 3427–3430. d) A. Chardon, O. Maubert, J. Rouden, J. Blanchet, *ChemCatChem* **2017**, *9*, 4460–4464. e) J. Jeong, K. Suzuki, K. Yamaguchi, N. Mizuno, *New J. Chem.* **2017**, *41*, 13226–13229. f) R. Rubio-Presa, M. A. Fernández-Rodríguez, M. R. Pedrosa, F. J. Arnáiz, R. Sanz, *Adv. Synth. Catal.* **2017**, *359*, 1752–1757. g) S. Gupta, P. Sureshbabu, A. K. Singh, S. Sabiah, J. Kandasamy, *Tetrahedron Lett.* **2017**, *58*, 909–913. h) K. D. Kim, J. H. Lee, *Org. Lett.* **2018**, *20*, 7712–7716. i) M. O. Konev, L. Cardinale, A. Jacobi Von Wangelin, *Org. Lett.* **2020**, *22*, 1316–1320. j) H. Tinnermann, S. Sung, B. A. Cala, H. J. Gill, R. D. Young, *Organometallics* **2020**, *39*, 6, 797–803. k) J. H. An, K. D. Kim and J. H. Lee, *J. Org. Chem*.**2021**, *86*, 2876–2894

[7] For selected examples on the use of heteroaromatic *N*–oxides in C–H activation processes, see: a) L. C. Campeau, S. Rousseaux, K. Fagnou, *J. Am. Chem. Soc.* **2005**, *127*, 18020–18021. b) H. P. Kokatla, P. F. Thomson, S. Bae, V. R. Doddi, M. K. Lakshman, *J. Org. Chem.* **2011**, *76*, 7842–7848. c) X. Zhang, Z. Qi, X. Li, *Angew. Chemie - Int. Ed.* **2014**, *53*, 10794–10798. d) W. Jo, J. Kim, S. Choi, S. H. Cho, *Angew. Chemie - Int. Ed.* **2016**, *55*, 9690–9694. e) Z. Zhang, C. Pi, H. Tong, X. Cui, Y. Wu, *Org. Lett.* 2017, *19*, 440–443.

[8] a) J. Kim, C. R. Bertozzi, *Angew. Chemie - Int. Ed.* 2015, **54**, 15777–15781. b) T. Hirayama, H. Tsuboi, M. Niwa, A. Miki, S. Kadota, Y. Ikeshita, K. Okuda, H. Nagasawa, *Chem. Sci.* **2017**, *8*, 4858–4866.

[9] E. Howard, W. F. Olszewski, *J. Am. Chem. Soc.* **1959**, *81*, 1483–1484.

[10] (a) K. Tokumura, H. Goto, H. Kashiwabara, C. Kaneko, M. Itoh, *J. Am. Chem. Soc.* **1980**, *102*, 5643–5647. (b) for a recent article discussing the formation of oxaziridines through irradiation of pyridine N-oxides, see: (b) E. E. Hurlow, J. B. Lin, M. J. Dweck, S. Nuryyeva, Z. Feng, T. K. Allred, K. N. Houk and P. G. Harran*, J. Am. Chem. Soc*., **2020**, *142*, 20717–20724.

[11] B. Kempf, H. Mayr, *Chem. - A Eur. J.* **2005**, *11*, 917–927.

[12] M. Horn, L. H. Schappele, G. Lang-Wittkowski, H. Mayr, A. R. Ofial, *Chem. - A Eur. J.* **2013**, *19*, 249–263.

[13] A. M. Kirk, C. J. O'Brien, E. H. Krenske, *Chem*. *Commun*., **2020**, *56*, 1227-1230.

[14] For selected examples, see: a) M. Nappi, G. Bergonzini, P. Melchiorre, *Angew. Chemie - Int. Ed.* **2014**, *53*, 4921–4925. b) S. R. Kandukuri, A. Bahamonde, I. Chatterjee, I. D. Jurberg, E. C. Escudero-Adán, P. Melchiorre, *Angew. Chemie - Int. Ed.* **2015**, *54*, 1485–1489. c) J. Davies, S. G. Booth, S. Essafi, R. A. W. Dryfe, D. Leonori, *Angew. Chemie - Int. Ed.* **2015**, *54*, 14017–14021. e)T. Morack, C. Mück-Lichtenfeld, R. Gilmour, *Angew. Chemie - Int. Ed.* **2019**, *58*, 1208–1212. f) G. E. M. Crisenza, D. Mazzarella, P. Melchiorre, *J. Am. Chem. Soc.* **2020**, *142*, 5461–5476.

[15] a) A. Albini, M. Alpegiani, *Chem. Rev.* **1984**, *84*, 43–71; b) A. Albini, E. Fasani, A. M. Amer (**1995**) In: CRC handbook of organic photochemistry and photobiology. CRC Press, Boca Raton FL, pp 879-891; c) A. Albini, M. Fagnoni (**2004**) CRC handbook of organic photochemistry and photobiology, 2nd Edition. CRC Press, Boca Raton FL, pp 1-21. d) O. Larionov (Ed.) *Heterocyclic N-Oxides. Topics in Heterocyclic Chemistry*, **2017**, vol 53.

[16] C. Adamo, V. Barone, *J. Chem. Phys.*, **1999**, *110*, 6158-6170; W. J. Hehre, K. Ditchfield, J. A. Pople, *J. Chem. Phys.,* **1972**, *56*, 2257-2261; V. Barone, M. Cossi, *J. Phys. Chem. A.,* **1998**, *102*, 11, 1995-2001.

[17] F. Furche, R. Ahlrichs, *J. Chem. Phys.*, **2002**, *117*, 7433-7447.

[18] R. A. Marcus, *Annual Review of Physical Chemistry*, **1964**, *15*, 155-196.

[19] M. Besora, P. Vidossich, A. Lledos, G. Ujaque, F. Maseras, *J. Phys. Chem. A* **2018**, *122*, 1392-1399.

Entry for the Table of Contents

This work describes efficient metal-free approaches for chemoselective deoxygenation of amine N-oxides. Scope and reaction mechanisms of these reactions are discussed.